



Heterogeneous Fenton-like oxidative degradation of sulfanilamide catalyzed by RuO₂-rectorite composite

Feifei Pan¹ · Jianhong Yang¹ · Jun Cai² · Lianye Liu¹

Received: 17 February 2021 / Accepted: 15 July 2021

© The Author(s), under exclusive licence to Springer Nature B.V. 2021

Abstract

RuO₂-rectorite (RuO₂-Rec) was prepared by intercalation, deposition and calcination. Its structure was characterized by XRD, XPS, SEM and EDS. It was used as a catalyst for the sulfanilamide (SA) degradation in the presence of H₂O₂. Unlike sodium-rectorite and RuO₂ which couldn't catalyze the degradation of SA, RuO₂-Rec could effectively catalyze the decomposition of H₂O₂ into hydroxyl radicals to degrade SA. The degradation rate could reach ~100% under the optimal conditions of 58 μmol/L of SA, 1.16 mmol/L of H₂O₂, 0.133 g/L of RuO₂-Rec, pH 3.5 and 25 °C in 5 h. The degradation process conformed to pseudo-first-order kinetic correlation. This degradation was affected by pH, the amount of RuO₂-Rec and the concentrations of H₂O₂ and SA. However, under the optimal pH value of 3.5, a high degradation rate could be achieved with the increase in SA concentration from 58 μmol/L to 290 μmol/L as long as the optimal ratio of RuO₂-Rec, H₂O₂ and SA kept unchanged. In addition, RuO₂-Rec was stable and possessed low ruthenium leaching rate and excellent reusability. Therefore, RuO₂-Rec is expected to be an active catalyst for the pollutant removal in the heterogeneous Fenton-like system.

Keywords Rectorite · Ruthenium (IV) oxide · Catalytic oxidation · Sulfanilamide · Degradation

Introduction

Antibiotics are widely used in humans, veterinary medicine and aquaculture to prevent or treat microbial infections [1, 2]. So far, hundreds of different antibiotics have been used [3]. Sulfanilamide is one of these antibiotics, which is commonly used in

✉ Jianhong Yang
yangshenyang3@163.com

¹ School of Environmental and Safety Engineering, Changzhou University, Changzhou 213164, China

² Key Laboratory of Fermentation Engineering (Ministry of Education), Hubei University of Technology, Wuhan 430068, China

animal husbandry to control bacterial diseases [4–8]. However, its metabolic rate in the body is very low, and most of it is discharged into the environment in its original form. The concentrations of sulfanilamide in pig slurry, surface water, groundwater and purified waste water were found to be up to 500 mg/L, 0.04 µg/L, 0.02 µg/L and 1.0 µg/L, respectively [3, 9]. Because of its good stability, it is difficult to degrade and remove naturally and it accumulates excessively in the aquatic environment, which not only results in the drug resistance of bacterial pathogens and seriously threatens human and animal health, but also affects chlorophyll synthesis, enzyme secretion and root growth of plants [10–13]. Therefore, the removal of sulfanilamide from wastewater has attracted much attention.

As an advanced oxidation process to remove sulfonamides and their derivatives, Fenton reaction has been extensively studied in wastewater treatment [14, 15]. In homogeneous Fenton system, iron ion is used as catalyst to decompose the hydrogen peroxide (H_2O_2) into hydroxyl radicals ($\cdot\text{OH}$) at pH 2–4 and $\cdot\text{OH}$ effectively destroys sulfonamides to CO_2 , H_2O and inorganic ions [14, 16, 17]. Although the homogeneous Fenton system is highly efficient, the stoichiometric requirements of Fe^{2+} have a very negative impact on Fenton chemistry as a solution for pollutant remediation. One alternative to stoichiometric Fe^{2+} is the use of UV-photo-Fenton reaction [18–20]. Due to the existence of UV light, the conversion of Fe^{3+} to Fe^{2+} with low concentration is also realized. However, the wastewater is usually opaque and most organic compounds show strong absorption band in the ultraviolet region, which hinders the absorption of photons by low concentration Fe^{3+} [21]. These limit the application of UV-photo-Fenton reaction in the wastewater treatment. In order to solve the problems mentioned above, the development of heterogeneous Fenton-like system that can take place in the dark has become the focus of attention.

Considering that Fenton reaction is mainly promoted by iron and copper ions, iron and copper oxides are usually used as solid catalysts for heterogeneous Fenton-like systems. Iron oxide showed the best catalytic performance for the degradation of organic pollutants at pH 3–4 [22, 23]. Obviously, the leaching of iron ion was inevitable under such conditions due to its alkaline oxide characteristics. Feng et al. [23] found that for the degradation of sulfanilamide, $\text{CuO}/\text{H}_2\text{O}_2$ oxidation was best at pH 6.5 and CuFe_2O_4 nanoparticle also showed good catalytic effect under neutral conditions due to the existence of copper ions. However, although CuO and CuFe_2O_4 nanoparticles revealed relative stability under neutral conditions, metal leaching still existed. For the CuFe_2O_4 nanoparticles, the leaching amount of copper ion was much higher than that of ferric ion. In order to improve the stability of catalysts, iron and copper oxides were usually deposited on the supporter as solid catalysts for heterogeneous Fenton-like system [21, 24]. A convenient and important way was to immobilize iron and copper oxides on clays. Iron and copper oxides pillared layered aluminosilicates (clays) (Fe/Al - and Cu/Al - PILCs) showed high catalytic activity in Fenton oxidation of organic pollutants. Making use of Fe/Al -PILCs as catalyst in Fenton-like system, the removal rate of sulfanilamide with H_2O_2 was 95–99% at pH 3.1 and 4.1 for 6 h [25]. Achma et al. [26] reported that Cu/Al -PILCs showed high catalytic activity for the H_2O_2 oxidation of tyrosol. When 500 mg/L of catalyst was used, total conversion of 500 mg/L tyrosol was achieved in 1 h at 40 °C with stoichiometric amount of H_2O_2 . Three metal oxides $\text{Fe}/\text{Cu}/\text{Al}$ -PILCs had also

been prepared and used as heterogeneous Fenton-like catalyst, which showed good catalytic degradation effect on phenol and sulfanilamide [8, 18]. However, even if oxides of iron and copper were anchored to the aluminum pillars, metal leaching was inevitable at pH 2–4 because they are alkaline oxides. This often caused a prominent reduction in the catalytic activity of these catalysts after being reused for 2–5 times [8, 18, 25, 26]. So far, people have been looking for new catalysts for the heterogeneous Fenton-like reaction system.

Ruthenium, a transition metal, is located in Group VIII B of the Periodic Table like iron. However, unlike iron oxides, RuO_2 is an acidic oxide and insoluble in acid solution. RuO_2 was often loaded on various carriers and used as electrode materials and catalysts for sensors [27], supercapacitors [28, 29], water splitting [30–32] and oxidation of organic compounds [33]. In the field of environmental applications, RuO_2 had been deposited on the surfaces of TiO_2 for photocatalytic degradation of pollutants in water [34, 35] and for the catalytic total oxidation of volatile organic compounds [36]. Co-loaded RuO_2 and Pt on the t-Ba TiO_3 showed a synergistic enhancement effect on the piezo-degradation of tricyclazole [37]. However, RuO_2 as a solid catalyst for heterogeneous Fenton-like reactions hasn't been hitherto reported. Recently, it has been confirmed that protein-supported RuO_2 nanoparticles can catalyze the decomposition of H_2O_2 into $\cdot\text{OH}$ [38]. In addition, rectorite is a layered clay mineral, which consists of alternating pairs of dioctahedral mica-like layer and dioctahedral smectite-like layer at ratio of 1:1 [39]. Because of its cation exchange capacity, adsorptive capacity, good hydrophilicity and excellent dispersibility in water, it was often used to support catalysts in aqueous solution [40–45]. Liu et al. [43] immobilized CuO on rectorite to achieve efficient aerobic oxidation of alcohol in water. It was reported that loading (N, Cu) co-doped TiO_2 [41], Ag_2O [46] and nano- Fe_3O_4 [47] on rectorite, respectively, could also effectively improve their catalytic degradation performances for organic pollutants and their stability in aqueous solution. In this study, RuO_2 was loaded on rectorite and used as a heterogeneous catalyst for Fenton-like reaction. Its catalytic performance was evaluated by the degradation of sulfanilamide (SA) in aqueous solution and compared with sodium-rectorite and RuO_2 . Furthermore, the active species produced in the degradation reaction, the degradation kinetics, the factors affecting the catalytic degradation and the reusability of RuO_2 -Rec were also investigated.

Experimental

Materials

Calcium-rectorite (Ca-Rec) was from Hubei Zhongxiangmingliu Development Co., Ltd (China). Its element composition is listed in Table 1. Ruthenium trichloride hydrate and ruthenium (IV) oxide were purchased from Shanghai Macklin Biochemical Co., Ltd (China). Sulfanilamide and hydrogen peroxide (30%) were obtained from Sinopharm (China). Ruthenium standard solution (1000 $\mu\text{g}/\text{mL}$) was purchased from Guobiao (Beijing) Testing & Certification Co. Ltd. (GBTC, China). All other chemicals were used as received.

Table 1 Contents of various elements in rectorite samples based on the EDS analysis

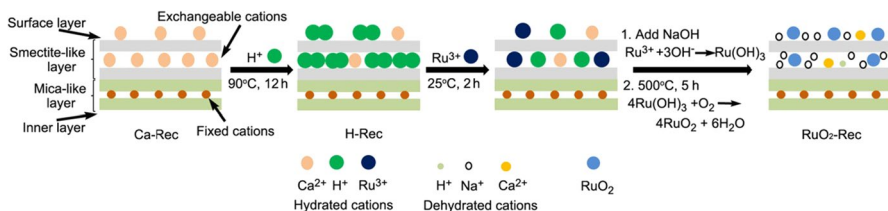
| Sample | Content of element (wt%) | | | | | | | | | | | |
|-----------------------|--------------------------|-------|-------|------|------|-------|-------|------|------|------|------|------|
| | Ru | C | O | Na | Mg | Al | Si | S | K | Ca | Ti | Fe |
| Ca-Rec | 0 | 12.73 | 55.15 | 0.66 | 0.21 | 12.84 | 13.66 | 0.51 | 0.55 | 1.66 | 1.27 | 0.95 |
| H-Rec | 0 | 0 | 63.10 | 1.07 | 0.23 | 15.00 | 17.04 | 0.28 | 0.82 | 1.16 | 1.01 | 0.28 |
| RuO ₂ -Rec | 9.59 | 0 | 61.05 | 0.87 | 0.19 | 12.33 | 13.57 | 0 | 0.53 | 0.90 | 0.97 | 0 |

Preparation of RuO₂-rectorite composite

Ca-Rec was first modified by acid treatment. 10 g of Ca-Rec was dispersed into 150 ml of HCl (1.2 mol/L) and stirred at 90 °C for 12 h. The stirring speed was maintained at 280 rpm. After standing overnight, the mixture was centrifuged at 4000 rpm ($\times 2,900$ g). The precipitate was washed with H₂O until no chloride ions were detectable. The washing was repeated approximately 30 times. The acidified rectorite (H-Rec) was obtained after drying at 90 °C. Then 5 g of H-Rec was dispersed in 150 mL water, and 250 mL of 0.01 mol/L ruthenium chloride aqueous solution was put in. The mixture was stirred at 25 °C for two hours. Then 0.2 mol/L of NaOH was added dropwise to maintain pH at 5.5–6.5. After 24 h, the suspension was filtrated. The precipitate was rinsed with H₂O, dried at 90 °C and then calcined at 500 °C for five hours. The product RuO₂-rectorite composite was abbreviated to RuO₂-Rec. The preparation process is illustrated in Scheme 1. In addition, sodium-rectorite (Na-Rec) was also prepared by using H-Rec. 1 g of H-Rec was dispersed in 100 mL of NaCl solution (1.2 mol/L) and stirred at 80 °C for 10 h. The mixture was centrifuged and the precipitate was washed with H₂O until no chloride ions were detectable. Na-Rec was obtained after drying at 105 °C for 5 h.

Characterization

The XRD patterns were recorded on a Rigaku D/max 2500 PC X-ray diffractometer (Japan) with a Cu-target tube ($\lambda = 1.5406 \text{ \AA}$). The test was carried out at 40 kV of voltage and 100 mA of current. The scan range was $2\theta = 2\text{--}70^\circ$. The surface morphology and element distribution of samples were observed and recorded on a Zeiss SUPRA 55 field emission scanning electron microscope equipped with QUANTAX



Scheme 1 The Preparation process of RuO₂-Rec. In the surface of RuO₂-Rec, part of RuO₂ came from Ru(OH)₃ deposited on the surface of Rec from the solution when NaOH was added

energy-dispersive X-ray spectrometer (Germany). XPS was analyzed using an ESCALAB 250XI spectrometer (Thermo, USA).

Catalytic oxidative degradation of sulfanilamide

The catalytic oxidative degradation of SA was carried out in a glass flask equipped with a magnetic stirrer at 25 °C. RuO₂-Rec was added into 30 mL of SA aqueous solution with a certain pH. After stirring for 10 min, 35 μL of H₂O₂ aqueous solution with appropriate concentration was added to start the reaction. The amount of RuO₂-Rec, the concentration of SA aqueous solution and the molar ratio of H₂O₂ to SA were controlled in the range of 0.033–0.233 g/L, 58–290 μmol/L (10–50 mg/L) and 2.5:1–100:1, respectively. The pH of the solution was controlled at 2.5–6.5 by adding 0.2 mol/L of NaOH and 3.0 mol/L of H₂SO₄. During the reaction process, the solution was detected using a Shimadzu LC-20AT HPLC (Japan) equipped with an InertSustain C18 (250 mm×4.6 mm) column (GL Sciences, Japan) at 258 nm. The column temperature, the eluent and the flow rate were 35 °C, a mixture of water and acetonitrile (v/v, 4:1) and 1.0 mL/min, respectively. Meanwhile, the reaction solution was also monitored by a Shimadzu 1601 UV–Vis spectrometer (Japan), and TOC in the solution was measured using a Multi N/C 2100s analyzer (Analytik Jena, Germany). The experiments were triplicate. For comparison, the catalytic properties of Na-Rec and pure RuO₂ were also investigated. In addition, under pH 3.5 and 25 °C, 3.0 mg of RuO₂-Rec (or Na-Rec) and 30 mL of SA aqueous solution (58 μmol/L) were mixed and stirred. The adsorption of RuO₂-Rec (or Na-Rec) for SA was evaluated.

Leaching test of ruthenium ion

Under pH 3.5 and 25 °C, 4.0 mg of RuO₂-Rec and 30 mL of SA aqueous solution (58 μmol/L) were mixed. After 5-h reaction, the solution was filtered. Nitric acid was added to the filtrate until its concentration was 2 wt%. Then the concentration of ruthenium ion was determined by NexION 350X ICP-Mass spectrometer (PerkinElmer, USA). Calibration curve was made using ruthenium standard solution.

Results and discussion

Characterization of RuO₂-rectorite composite

Generally, in order to realize the substitution of calcium ions in Ca-rectorite by other metal ions, a preferential acid activation is necessary. Here, Ca-Rec was first activated in 1.2 mol/L of HCl at 90 °C for 12 h, and then Na⁺ and Ru³⁺ ions were introduced into rectorite, respectively (see Scheme 1). Figure 1a shows the XRD patterns of original rectorite and its modified products. After Ca-Rec was acidified, its basal reflection at $2\theta=3.541^\circ$ shifted to $2\theta=3.560^\circ$, and its basal spacing decreased from 2.493 to 2.480 nm. The decrease in the basal spacing indicated

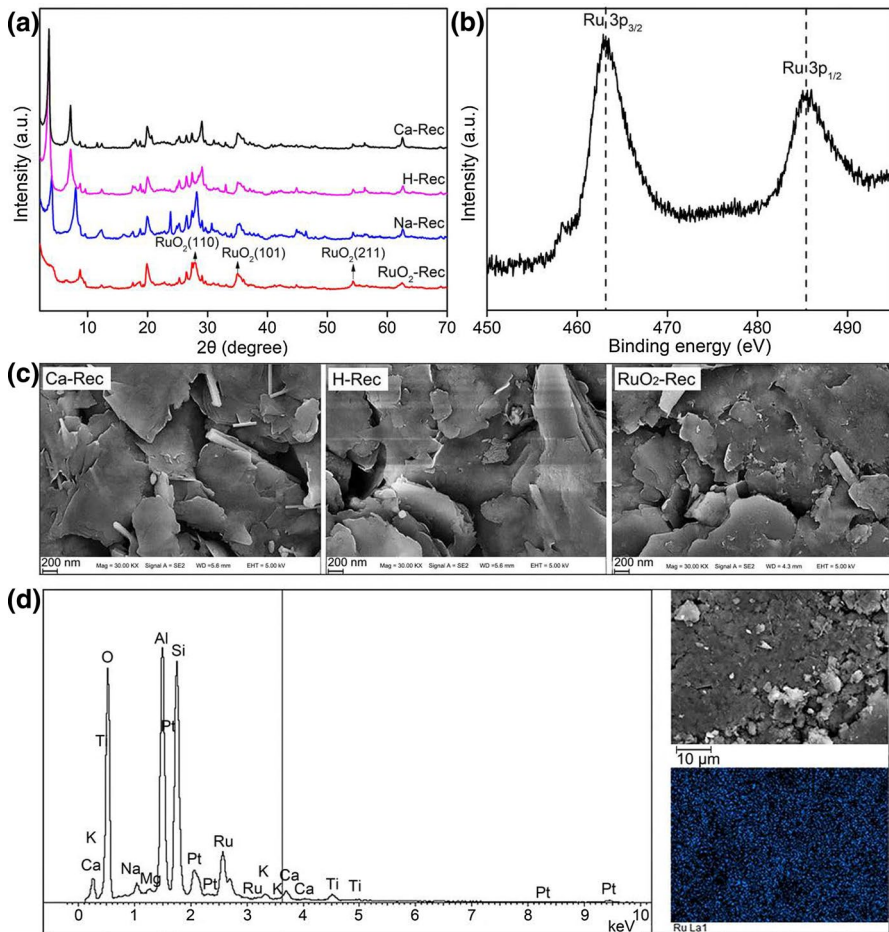


Fig. 1 **a** XRD patterns of Ca-Rec, H-Rec, Na-Rec and RuO₂-Rec; **b** Ru 3p XPS spectra of RuO₂-Rec; **c** SEM images of Ca-Rec, H-Rec and RuO₂-Rec; **d** quantitative analysis and element mapping of Ru by SEM-EDS of RuO₂-Rec

that H⁺ had been introduced into the interlayer of rectorite [48–50]. Moreover, the results of EDS analysis showed that the content of Ca element decreased from 1.66 to 1.16 wt%, further suggesting that some Ca²⁺ in Ca-rectorite had been replaced by H⁺ after acid treatment. Further, after H-Rec was treated with NaCl solution, the basal reflection was shifted to $2\theta=4.0^\circ$, and its basal spacing decreased to 2.207 nm. This decrease indicated that Na⁺ had been introduced into the interlayer of rectorite [42, 51]. After H-Rec was treated with ruthenium chloride solution, its basal reflection further shifted to $2\theta=3.989^\circ$ and its basal spacing also decreased to 2.213 nm. The intensity of the reflection also became very weak. These indicated that Ru³⁺ ions had been introduced into the interlayer of rectorite. In addition, when the pH value was adjusted to 5.5–6.5, Ru³⁺ was converted to Ru(OH)₃, and the Ru³⁺

in the solution was partly deposited on the surface of Rec in the form $\text{Ru}(\text{OH})_3$. Then Ru-rectorite was calcined at 500 °C for 5 h. Under such calcination, stable RuO_2 would be formed because of oxidation of oxygen [52] (see Scheme 1). In the XRD pattern of RuO_2 (Fig. 1a), there are three characteristic reflections $2\theta=28^\circ$, 35.1° and 54.1° assigned to RuO_2 (110), RuO_2 (101) and RuO_2 (211), respectively [36, 53–55]. In comparison with the XRD pattern of H-Rec, a new strong reflection at $2\theta=28^\circ$ appeared in the XRD pattern of RuO_2 -Rec, and the intensities of two reflections at $2\theta=35.1^\circ$ and 54.1° also increased from 2008 to 2390 and from 619 to 1017, respectively. These indicated that RuO_2 was loaded on the rectorite. Furthermore, RuO_2 -Rec was also characterized by XPS (Fig. 1b). For RuO_2 -Rec, the binding energy value of Ru ($3p_{3/2}$) was 463.1 eV, which was exactly the same as that of Ru^{4+} in the literature [56, 57]. This further indicated that Ru element existed on the rectorite in the RuO_2 species.

The results of SEM and EDS analysis of rectorite samples are shown in Fig. 1c and d. All of them showed a typical layered structure (Fig. 1c), indicating that acid treatment and the loading of RuO_2 did not affect the layered structure of rectorite. The EDS analysis showed that the content of Ru element in RuO_2 -Rec was 9.59 wt% (Table 1), indicating RuO_2 deposited on the surface of rectorite. The elemental mapping analysis by EDS showed RuO_2 was evenly distributed over the rectorite's surface (Fig. 1d). In addition, there was 12.73 wt% of carbon element in Ca-Rec (Table 1), but it disappeared after acid treatment, suggesting carbon element in the rectorite existed in the form of carbonate. Ca-Rec also contained a small amount of Ti element, which was also confirmed by the Ti ($2p_{1/2}$) peak at 458.6 eV of binding energy value in XPS spectrum (Fig. 1b) [58, 59]. No copper was detected in the rectorite sample. There was a small amount of Fe element in Ca-Rec (0.95 wt%) and H-Rec (0.28%). However, the Fe element was completely removed during the loading of RuO_2 (Table 1 and Fig. 1d). Therefore, when RuO_2 -Rec was used as the catalyst for the heterogeneous Fenton-like reaction, there was no interference from copper and iron ions.

Catalytic degradation performance of RuO_2 -rectorite composite

The catalytic degradation of sulfanilamide by RuO_2 -rectorite composite was evaluated under 25 °C, pH 3.5, 58 $\mu\text{mol/L}$ of SA, 1.16 mmol/L of H_2O_2 and 0.1 g/L of RuO_2 -Rec. The results are shown in Fig. 2a. It is observed that the concentration of sulfanilamide decreased swiftly with increasing the reaction time. 88.7% of sulfanilamide was removed in 5 h. The reaction process was tracked by HPLC (Fig. 2b). In the HPLC profiles, the peak at 4.21 min was related to the sulfanilamide. The intensity of the peak declined rapidly as the reaction time increased, further indicating the sulfanilamide was effectively removed under such conditions. At the same time, the degradation of sulfanilamide without RuO_2 -rectorite was investigated as well (Fig. 2a). It showed that in the absence of RuO_2 -rectorite, only 5.1% of sulfanilamide was removed in 5 h. This indicated that H_2O_2 itself could also react with SA to cause its degradation, but the degradation rate was very slow. In addition, considering that the amino group of sulfanilamide existed in the form of NH_3^+ under

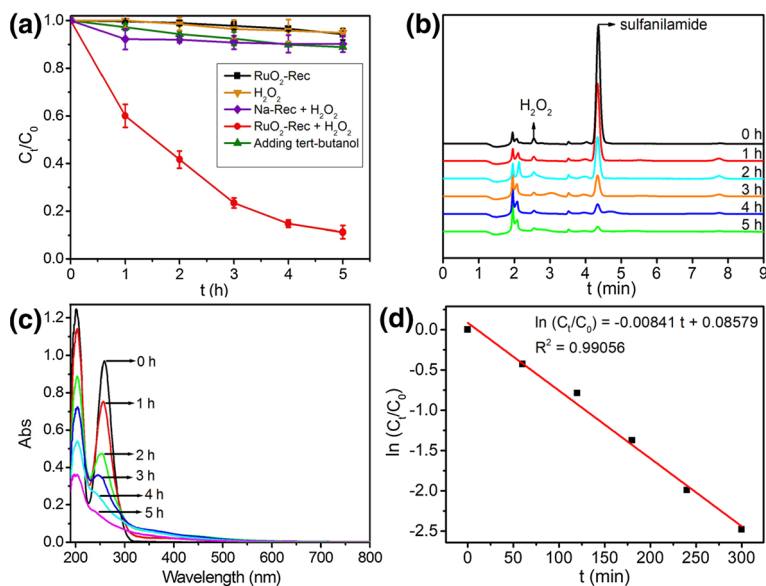


Fig. 2 **a** The removal of SA in the presence of H₂O₂ and RuO₂-Rec (\bullet), H₂O₂ without RuO₂-Rec (\blacktriangledown), H₂O₂, RuO₂-Rec and tert-butanol (\blacktriangle), and H₂O₂ and Na-Rec (\blacklozenge), and the absorption of SA by RuO₂-Rec in the absence of H₂O₂ (\blacksquare); **b** HPLC profiles of reaction solution in the degradation process of SA; **c** UV-Vis spectra of the reaction solution in the degradation process of SA; **d** the kinetic curve plotted as $\ln(C_t/C_0)$ versus time for the catalytic degradation of SA. Reaction conditions: 25 °C, pH 3.5, 10 mg/L SA (58 μ mol/L), 1.16 mmol/L H₂O₂ and 0.1 g/L RuO₂-Rec or Na-Rec. In addition, C_0 and C_t are the concentration of SA at 0 h and t h, respectively

acidic condition and it could be adsorbed by rectorite, the adsorption properties of the catalyst RuO₂-Rec were evaluated at 3.5 of pH. But only a small amount of sulfanilamide was adsorbed by the RuO₂-Rec and its removal rate was 5.7% in 5 h by adsorption (Fig. 2a). These results indicated that RuO₂-Rec had a significant catalytic effect on the oxidative degradation of sulfanilamide with H₂O₂.

Active species in catalytic degradation and possible degradation mechanism

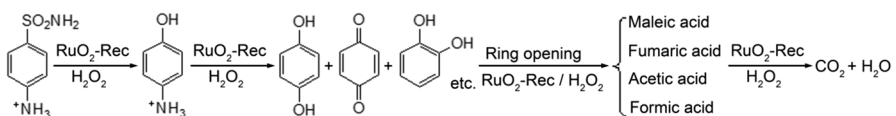
In the HPLC profiles, the peak at 2.56 min was related to H₂O₂ (Fig. 2b). The intensity of the peak decreased with the degradation of the sulfanilamide and 65.5% of H₂O₂ was consumed in 5 h, indicating that H₂O₂ was involved in the degradation process. Further, the active species in the degradation reaction was investigated. Tert-butanol was added into the reaction solution to trap the active species and its initial concentration was 11.6 mmol/L. The results showed that addition of tert-butanol greatly reduced the degradation rate of sulfanilamide and only 11.2% of sulfanilamide was removed in 5 h (Fig. 2a). Because tert-butanol was mainly used to trap the generated hydroxyl radicals (\cdot OH) [60], it could be inferred that \cdot OH was the active species in the reaction system, which was consistent with the results of protein-supported RuO₂ nanoparticles catalyzing the

decomposition of H_2O_2 to produce $\cdot\text{OH}$ [38]. Thus, the degradation of sulfanilamide could be considered as the result of Fenton-like reaction.

For the Fenton-like degradation of sulfanilamide, it was generally believed that it was subject to the cleavage of C-N, N-S and C-S bonds [23, 25]. Some intermediates such as phenol, catechol, resorcinol, hydroquinone, maleic acid, fumaric acid, acetic acid and formic acid were formed in the reaction process, and finally, SA was completely mineralized [23, 25]. We tracked the degradation process of SA with UV-Vis spectrometer, and the results are shown in Fig. 2c. In the UV-Vis spectra, the adsorption bands at 203 nm and 259 nm were assigned to K-band and B-band of sulfanilamide [61]. In the first hour of the reaction, the absorption band at 259 nm shifted to 256 nm and its intensity decreased swiftly. Considering that the molar extinction coefficients (ϵ) of B bands of protonated aniline ($\text{C}_6\text{H}_5\text{NH}_3^+$, $\lambda_{\text{max}}=254$ nm) and benzenesulfonamide ($\text{C}_6\text{H}_5\text{SO}_2\text{NH}_2$, $\lambda_{\text{max}}=264.5$ nm) were $160 \text{ M}^{-1}\cdot\text{cm}^{-1}$ and $740 \text{ M}^{-1}\cdot\text{cm}^{-1}$ [61], respectively, it could be reasonably inferred that the degradation reaction began with the sulfonamido group and the C-S bond was cleaved preferentially, which was consistent with the results in the literature [23]. With further increase in reaction time, the intensities of B-band continued to decrease and a shoulder peak at ~ 290 nm appeared. It was considered to be due to the cleavage of C-N bond and the formation of catechol, resorcinol, hydroquinone and p-benzoquinone [23, 25]. In addition, with the decrease in B-band intensity, K-band intensity also decreases gradually. After 5 h, the K-band also became very weak, indicating the ring opening reaction of phenyl ring occurred. Although the degradation mechanism of SA had not been investigated in detail here, combined with the reaction of $\text{HO}\cdot$ with SA reported in the studies [23, 25], its possible degradation course is shown in Scheme 2.

Kinetics of catalytic degradation

The kinetic behavior of catalytic degradation of SA by $\text{RuO}_2\text{-Rec}$ was also investigated under 25°C , pH 3.5, $58 \mu\text{mol/L}$ of SA, 1.16 mmol/L of H_2O_2 and 0.1 g/L of $\text{RuO}_2\text{-Rec}$. According to the fitting experimental data, the degradation process conformed to pseudo-first-order kinetic correlation (Fig. 2d), which accorded with the pseudo-first-order kinetics of Fenton-like reactions reported in the literature [62]. Under the above experimental conditions, the fitting equation was $\ln(C/C_0) = -0.00841t + 0.08579$ (apparent rate constant $k = -0.00841 \text{ min}^{-1}$) and the correlation coefficient (R^2) was 0.99056.



Scheme 2 Possible degradation course of sulfanilamide

The role of rectorite and RuO₂

The role of rectorite and RuO₂ in the degradation of SA was also investigated. If RuO₂-Rec was replaced by 0.1 g/L of Na-Rec under the reaction conditions in the “Catalytic degradation performance of RuO₂-rectorite composite” section, the removal rate of sulfanilamide was only 9.8% in 5 h (Fig. 2a). In comparison with the degradation of SA by H₂O₂ itself (Fig. 2a) and the adsorption of SA by Na-Rec (6.2% of removal rate in 5 h), it could be found that rectorite had almost no catalytic activity for SA degradation in the presence of H₂O₂. When RuO₂-Rec was replaced by pure RuO₂, the removal rate of sulfanilamide was also very low (Fig. 3a). When the amount of RuO₂ was 0.003 g/L, the removal rate of SA was 4.7% in 5 h. As the amount of RuO₂ increased to 0.1 g/L, the removal rate of SA only increased to 20% in 5 h. However, the consumption rate of H₂O₂ increased rapidly with the increase in RuO₂ dosage (Fig. 3b). When the dosage of RuO₂ was 0.033 g/L and 0.1 g/L, H₂O₂ had been completely consumed in 0.5 h, while SA was only removed by 2.5% and 10.3%, respectively. Even though there was no H₂O₂ in the solution, the removal of SA increased gradually with the further increase in reaction time, and the removal rate of SA reached 9.4% and 20.0% at 5 h, respectively (Fig. 3b). In addition, the adsorption of SA by RuO₂ was also investigated (Fig. 3c). When the dosage of RuO₂ was 0.033 g/L and 0.1 g/L, it was found that 9.6% and 26.2% of SA were adsorbed by RuO₂ in 5 h, respectively. These results indicated that the removal of SA mainly resulted from the adsorption of RuO₂ and the rapid consumption of H₂O₂ did not contribute to the removal of SA.

Further, the dosage of RuO₂ was reduced to 0.013 g/L and 0.003 g/L. It was found that the consumption rate of H₂O₂ greatly declined, especially when 0.003 g/L of RuO₂ was used (Fig. 3b). However, different from RuO₂-Rec, the consumption of H₂O₂ was not in company with the catalytic degradation of SA by RuO₂ (Fig. 3a). In the presence of 0.013 g/L and 0.003 g/L of RuO₂, the removal rates of SA were only 3.4% and 4.7%, respectively. This indicated that H₂O₂ was not involved in the degradation of SA. It was speculated that for the pure RuO₂ particles, due to the concentration of catalytic active sites, H₂O₂ was rapidly

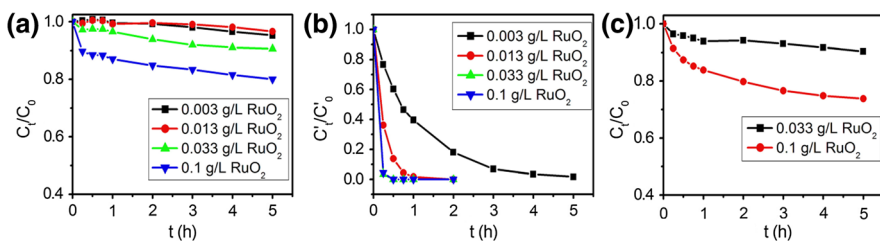
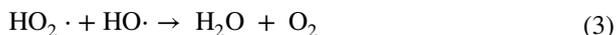
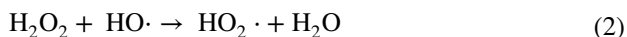


Fig. 3 **a** Effects of pure RuO₂ on the removal of SA; **b** effects of different amount of RuO₂ on H₂O₂ consumption; **c** removal of SA by RuO₂ in the absence of H₂O₂ (reaction conditions: 25 °C, pH 3.5, 58 μmol/L of SA, 1.16 mmol/L of H₂O₂ and 0.003–0.1 g/L of RuO₂). In addition, C₀ and C_t are the concentration of SA at 0 h and t h, respectively. C'₀ and C'_t are the concentration of H₂O₂ at 0 h and t h, respectively

decomposed into $\text{HO}\cdot$, high concentration of $\text{HO}\cdot$ was accumulated on the surface of RuO_2 , and then they were consumed swiftly via the following reactions [23, 25, 63, 64]:

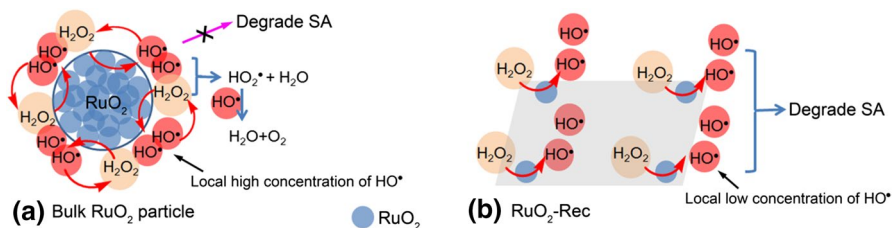


This resulted in the decomposition of H_2O_2 , but the degradation of SA was not initiated (Scheme 3a). However, for the RuO_2 -Rec, RuO_2 was uniformly distributed on the surface of rectorite as mentioned earlier (Fig. 1d). Due to the big distance between RuO_2 active sites, the concentration of produced $\text{HO}\cdot$ locally was not high enough, thus greatly reducing the consumption of $\text{HO}\cdot$ via the reactions (1)–(3). In this way, the hydroxyl radicals generated could react with SA and caused its degradation (Scheme 3b). Therefore, RuO_2 supported on rectorite could solve the problem that pure RuO_2 only decomposed H_2O_2 without degrading organic pollutants. Furthermore, it was possible that rectorite endowed RuO_2 with good hydrophilicity and excellent dispersibility in water [42, 43], which should be conducive to the catalytic degradation of SA by RuO_2 -Rec as well.

Influencing factors of catalytic degradation of sulfanilamide

Effect of pH

For Fenton-like systems, the pH of the reaction system strongly influenced the activity of the catalyst [8, 18, 22–26]. The effects of pH on the SA removal were investigated under 25 °C, 58 $\mu\text{mol/L}$ of SA, 0.1 g/L of RuO_2 -Rec and 1.16 mmol/L of H_2O_2 . The results are shown in Fig. 4a. The highest degradation efficiency of SA appeared at 3.5 of pH. The pH value was basically consistent with the reported heterogeneous Fenton systems with Fe/Cu/Al and (Al–Fe) pillared clays and nano- Fe_3O_4 /rectorite composite as catalysts [8, 25, 47]. The characteristic of these clays was assumed to be due to their special environment, which made them the best activity at this pH value [8]. In addition, it was observed in our experiment that the



Scheme 3 Possible interaction of pure RuO_2 **a** and RuO_2 -Rec **b** with H_2O_2

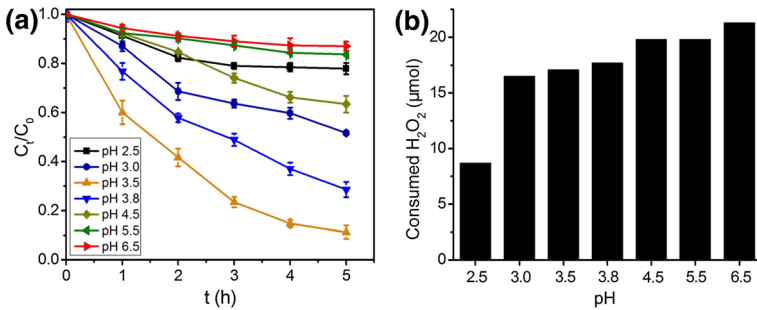


Fig. 4 Effects of pH value on sulfanilamide degradation **a** and H_2O_2 consumption **b**. Reaction conditions: 25 °C, pH 2.5–6.5, 58 $\mu\text{mol/L}$ of SA, 1.16 mmol/L of H_2O_2 and 0.1 g/L of $\text{RuO}_2\text{-Rec}$. C_0 and C_t are the concentration of SA at 0 h and t h, respectively

decomposition rate of H_2O_2 was accelerated with the increase in pH value from 2.5 to 6.5 (Fig. 4b). Obviously, the accelerated decomposition of hydrogen peroxide did not necessarily lead to the increase in SA degradation. This was because the HO· free radicals formed could be consumed via the reactions (1)–(3) as mentioned previously. Because these HO· radicals were not involved in the decomposition of SA, they did not contribute to the degradation of SA. Therefore, controlling the decomposition rate of H_2O_2 was a key to the degradation of SA. In this study, the decomposition rate of H_2O_2 was most suitable at pH 3.5.

Effects of H_2O_2 and SA concentrations

The effects of H_2O_2 concentration on the degradation of SA were investigated under 25 °C, pH 3.5, 58 $\mu\text{mol/L}$ of SA and 0.1 g/L of $\text{RuO}_2\text{-Rec}$. The results are shown in Fig. 5a. As the concentration of H_2O_2 and the molar ratio of H_2O_2 to SA increased from 0.145 to 2.32 mmol/L and from 2.5 to 40, respectively, the degradation rate of SA increased from 48.4% to 100% in 5 h. However, as the molar ratio of H_2O_2 to

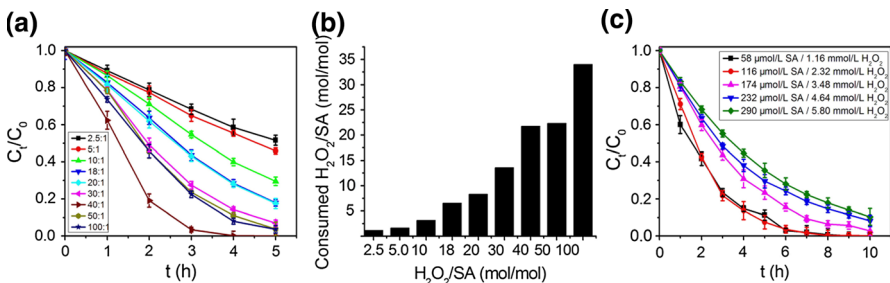


Fig. 5 **a** Effects of H_2O_2 concentration on the degradation of SA (58 $\mu\text{mol/L}$); **b** H_2O_2 consumption under different molar ratio of H_2O_2 to SA (58 $\mu\text{mol/L}$); **c** effects of H_2O_2 and SA concentrations on the degradation of SA under 20:1 molar ratio of H_2O_2 to SA. Reaction conditions: pH 3.5, 25 °C and 0.1 g/L of $\text{RuO}_2\text{-Rec}$. C_0 , C_t are the SA concentration at 0 h and t h, respectively

SA further increased, the degradation rate of SA decreased slightly. When the ratio was 100, the degradation rate of SA was 94.4% in 5 h. In theory, the molar ratio of H_2O_2 to SA is 18 for the full mineralization of SA [25]. From the point of view of H_2O_2 consumption within 5 h, the consumption of H_2O_2 gradually increased with the increase in molar ratio of H_2O_2 to SA (Fig. 5b). When the ratio of H_2O_2 to SA reached 40, the ratio of consumed H_2O_2 to SA exceeded 18. But further increase in H_2O_2 consumption led to a slight reduction in SA degradation. Actually, in addition to reacting with SA, the $\text{HO}\cdot$ free radicals formed by $\text{RuO}_2\text{-Rec}$ could be consumed by Eqs. (1)–(3). When the molar ratio of H_2O_2 to SA was less than 20:1, the $\text{HO}\cdot$ free radicals formed by $\text{RuO}_2\text{-Rec}$ could mainly interact with SA to leading to its degradation. Once the molar ratio exceeded 30:1, more $\text{HO}\cdot$ free radicals would be reacted with H_2O_2 molecules and be consumed, thus reducing the number of $\text{HO}\cdot$ free radicals in the reaction with SA. When the molar ratio of 100:1 was used, some gas production could be observed during the experiment as well. This could be due to the oxygen produced by the consumption of the $\text{HO}\cdot$ free radicals according to the reactions (2) and (3). In addition, when the molar ratio of H_2O_2 to SA was 20:1, complete degradation of SA could also be achieved by prolonging the reaction time to 9 h (Fig. 5c). Therefore, for the catalytic degradation of SA by $\text{RuO}_2\text{-Rec}$, it should be appropriate that the molar ratio of H_2O_2 to SA was kept at 20:1.

If the molar ratio of H_2O_2 to SA was kept at 20:1 with 0.1 g/L of $\text{RuO}_2\text{-Rec}$, and the concentration of SA was increased from 58 to 290 $\mu\text{mol/L}$, the degradation rate of SA decreased from 88.7 to 64.6% in 5 h (Fig. 5c). At the same time, the consumption of H_2O_2 decreased from 75.2 to 45.5% in 5 h. Obviously, this decrease in SA degradation with the increase in SA concentration was due to the formation of insufficient hydroxyl radicals. In order to improve the degradation rate of SA, the method of prolonging reaction time could be used. However, when the concentration of SA was 290 $\mu\text{mol/L}$, the reaction time was prolonged to 10 h and the degradation rate only reached 89.7%. Therefore, it was not a good method to increase the degradation rate only by prolonging the reaction time at high SA concentration.

Effect of catalyst

The effects of $\text{RuO}_2\text{-Rec}$ content on the degradation of SA were investigated under 25 °C, 3.5 of pH, 58 $\mu\text{mol/L}$ of SA and 1.16 mmol/L of H_2O_2 . The results are shown in Fig. 6a. When the concentration of catalyst increased from 0.033 to 0.133 g/L, the degradation rate of sulfanilamide increased rapidly. This was mainly due to the increase in hydroxyl radical formation by $\text{RuO}_2\text{-Rec}$ catalyst. However, further increase in catalyst content caused a slight decline in the SA degradation. As mentioned above, this could also be due to the formation of excessive hydroxyl radicals, resulting in side effects [23, 25]. Therefore, under such a reaction condition, the appropriate amount of catalyst is 0.133 g/L.

If the molar ratio of H_2O_2 to SA was kept at 20:1 and the amount of catalyst also increased proportionally with the increase in the concentration of SA from 58 to 290 $\mu\text{mol/L}$, it was found that all SA the degradation rates could reach almost 100% in 5 h (Fig. 6b). This could be mainly that the hydroxyl radicals were increased proportionally with the increase in catalyst. Obviously, compared with prolonging the reaction

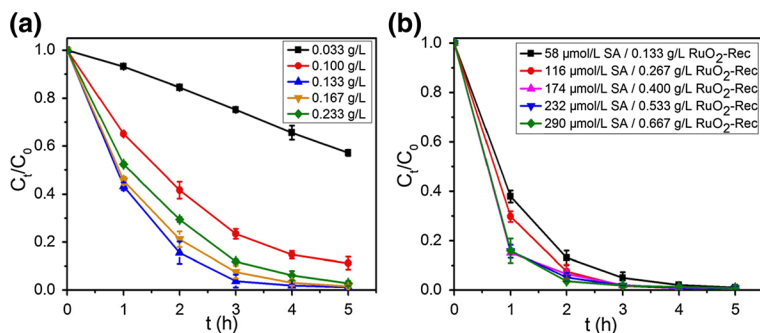


Fig. 6 Effects of RuO₂-Rec content on the SA degradation under 25 °C and 3.5 of pH. **a** 58 μmol/L of SA and 1.16 mmol/L of H₂O₂; **b** 20:1 molar ratio of H₂O₂ to SA remained unchanged and the amount of RuO₂-Rec increased proportionally with SA. C_0 and C_t are the concentration of SA at 0 h and t h, respectively

time, it was a better way for the SA degradation with high concentration to increase the amount of RuO₂-Rec.

Heterogeneous nature of catalyst and its recycling

In order to investigate whether leached ruthenium or RuO₂-Rec acted as a catalyst, the degradation of SA was carried out under 25 °C, pH 3.5, 58 μmol/L of SA and 0.133 g/L of RuO₂-Rec. After the solution was reacted for 5 h and the catalyst was filtered out, H₂O₂ and SA was added to achieve their initial concentration. The mixture continued to react for 5 h. It was observed that the degradation rate was only 7.8%. The result was basically consistent with that mentioned above which was from direct oxidation with hydrogen peroxide in the absence of RuO₂-Rec. These indicated that the SA degradation was heterogeneously catalyzed by RuO₂-Rec. In addition, ruthenium leaching from RuO₂-Rec was determined by ICP-MS spectrophotometry as well. The leaching amount of ruthenium was 0.30 μg/L in 5 h. It was obvious that the leached ruthenium was not enough to catalyze the degradation of SA. Meanwhile, in comparison with CuO, CuFe₂O₄ nanoparticle, Fe/Al-PILCs, Cu/Al-PILCs and Fe/Cu/Al-PILCs, the leaching amount of ruthenium from RuO₂-Rec was far less than that of Fe or Cu from these catalysts [8, 18, 23, 25, 26]. Further, for the heterogeneous Fenton-like system, the recyclability of RuO₂-Rec was also investigated under 25 °C, pH 3.5, 58 μmol/L of SA, 1.16 mmol/L H₂O₂ and 0.133 g/L of RuO₂-Rec (Table 2). After reaction for 5 h, RuO₂-Rec was separated by centrifugation, washed with water and dried at 90 °C for 2 h for the next use. It was observed that the activity of the recycling RuO₂-Rec was only very slightly decreased in four consecutive cycles, which could be due to the

Table 2 The recyclability of RuO₂-Rec

| Number of reuse | 1 | 2 | 3 | 4 |
|---------------------------------------|-------|-------|------|------|
| Degradation rate of sulfanilamide (%) | 100.0 | 100.0 | 98.2 | 98.1 |

fact that ruthenium was difficult to leach in the reaction process. These indicated that RuO₂-Rec had excellent stability and reusability.

Removal of TOC

The TOC change in the solution was investigated under 25 °C, pH 3.5, 0.133 g/L RuO₂-Rec, 1.16 mmol/L H₂O₂ and 58 μmol/L of SA. Although SA was completely removed in 5 h (Fig. 6a, b), it was found that only 17.0% of TOC removal was achieved. At this time, the consumption of H₂O₂ was 76.7%. When the reaction time was further prolonged to 11 h, H₂O₂ was completely consumed, but the removal rate of TOC was only 32.8%. After adding the same amount of H₂O₂ and repeating the above process for three times, the TOC value was finally reduced to 0. Obviously, a large amount of H₂O₂ was consumed ineffectively in the reaction process. This should be related to the fact that the amount of RuO₂ deposited on the rectorite and its distribution on the rectorite surface were not optimized.

Conclusions

In this paper, RuO₂-Rec was prepared and used in a heterogeneous Fenton-like system. RuO₂ supported on rectorite solved the problem that pure RuO₂ only catalyzed decomposition of H₂O₂ without degrading organic pollutants. RuO₂-Rec could effectively catalyze the degradation of sulfanilamide in the presence of H₂O₂. This degradation was affected by many factors, such as pH, the amount of RuO₂-Rec and the concentration of H₂O₂ and SA. In order to achieve excellent degradation efficiency, in addition to keeping the optimal pH at 3.5, the control of the ratios of H₂O₂, SA and RuO₂-Rec was particularly important. In addition, Ru was hardly leached in the reaction process and RuO₂-Rec possessed excellent reusability as well. However, although RuO₂-Rec could be a promising catalyst for the pollutant removal, the preparation of RuO₂-Rec still needs to be optimized to realize the effective utilization of H₂O₂.

Acknowledgements This work was supported by the Key Laboratory of Fermentation Engineering (Ministry of Education) and Hubei Key Laboratory of Industrial Microbiology Open Foundation in Hubei University of Technology.

Declarations

Conflict of interest The authors declare no conflict of interests.

References

1. A.B.A. Boxall, P. Blackwell, R. Cavallo, P. Kay, J. Tolls, *Toxicol. Lett.* **131**(1–2), 19 (2002)
2. B. Schmidt, J. Ebert, M. Lamshoft, B. Thiede, R. Schumacher-Buffel, R. Ji, P.F.-X. Corvini, A. Schäffer, *J. Environ. Sci. Health B* **43**(1), 8 (2008)
3. K. Kümmerer, *Chemosphere* **75**(4), 417 (2009)

4. R.H. Gustafson, R.E. Bowen, *J. Appl. Microbiol.* **83**(5), 531 (1997)
5. A.B.A. Boxall, L.A. Fogg, P. Blackwell, P. Kay, E.J. Pemberton, A. Croxford, *Rev. Environ. Contam. Toxicol.* **180**, 1 (2004)
6. J. Heise, S. Höltge, S. Schrader, R. Kreuzig, *Chemosphere* **65**(11), 2352 (2006)
7. A. Göbel, C.S. McArdeell, A. Joss, H. Siegrist, W. Giger, *Sci. Total Environ.* **372**(2–3), 361 (2007)
8. STs. Khankhasaeva, ETs. Dashinamzhiлова, D.V. Dambueva, *Appl. Clay Sci.* **146**, 92 (2017)
9. T. Wang, Y. Zhou, S. Cao, J. Lu, Y. Zhou, *Ecotox. Environ. Safe.* **172**, 334 (2019)
10. W. Baran, J. Sochacka, W. Wardas, *Chemosphere* **65**(8), 1295 (2006)
11. M. Crane, C. Watts, T. Boucard, *Sci. Total Environ.* **367**(1), 23 (2006)
12. Y. Xu, W. Yu, Q. Ma, H. Zhou, *Sci. Total Environ.* **530–531**, 191 (2015)
13. H. Li, B. Li, J. Ma, J. Ye, P. Guo, L. Li, *Chem. Eng. J.* **337**, 584 (2018)
14. W. Li, V. Nanaboina, Q. Zhou, G.V. Korshin, *Water Res.* **46**, 403 (2012)
15. R. Rodríguez, J.J. Espada, M.I. Pariente, J.A. Melero, F. Martínez, R. Molina, *J. Clean. Prod.* **124**, 21 (2016)
16. S. Dehghani, A.J. Jafari, M. Farzadkia, M. Gholami, *Iran. J. Environ. Health* **10**, 29 (2013)
17. J.-F. Yang, S.-B. Zhou, A.-G. Xiao, W.-J. Li, G.-G. Ying, *J. Environ. Sci. Health B* **49**(12), 909 (2014)
18. O. Gonzalez, C. Sans, S. Esplugas, *J. Hazard. Mater.* **146**(3), 459 (2007)
19. A.P.S. Batista, R.F.P. Nogueira, *J. Photochem Photobiol. A* **232**, 8 (2012)
20. A.P.S. Batista, B.A. Cottrell, R.F.P. Nogueira, *J. Photochem Photobiol. A* **274**, 50 (2014)
21. S. Navalon, M. Alvaro, H. Garcia, *Appl. Catal. B-Environ.* **99**, 1 (2010)
22. J.C. Barreiro, M.D. Capelato, L. Martin-Neto, H.C.B. Hansen, *Water Res.* **41**, 55 (2007)
23. Y. Feng, C. Liao, K. Shih, *Chemosphere* **154**, 573 (2016)
24. L.-A. Galeano, M.Á. Vicente, A. Gil, *Catal. Rev.* **56**(3), 239 (2014)
25. STs. Khankhasaeva, D.V. Dambueva, ETs. Dashinamzhiлова, A. Gil, M.A. Vicente, M.N. Timofeeva, *J. Hazard. Mater.* **293**, 21 (2015)
26. R.B. Achma, A. Ghorbel, A. Dafinov, F. Medina, *Appl. Catal. A-Gen.* **349**, 20 (2008)
27. R.M.A. Tehrani, S. Beyzavi, *Sensor. Mater.* **26**(9), 687 (2014)
28. H. Li, X. Li, J. Liang, Y. Chen, *Adv. Energy Mater.* **9**(15), 1803987 (2019)
29. S. Jeon, J.H. Jeong, H. Yoo, H.K. Yu, B.-H. Kim, M.H. Kim, *A.C.S. Appl. Nano Mater.* **3**(4), 3847 (2020)
30. H. Yoo, K. Oh, Y.R. Lee, K.H. Row, G. Lee, J. Choi, *Int. J. Hydrogen Energy.* **42**(10), 6657 (2017)
31. M.E.C. Pascuzzi, A. Goryachev, J.P. Hofmann, E.J.M. Hensen, *Appl. Catal. B-Environ.* **261**, 118225 (2020)
32. H. Sun, J.-M. Yang, J.-G. Li, Z. Li, X. Ao, Y.-Z. Liu, Y. Zhang, Y. Li, C. Wang, *J. Tang, Appl. Catal. B-Environ.* **272**, 118988 (2020)
33. T. Sreethawong, Y. Yamada, T. Kobayashi, S. Yoshikawa, *J. Mol. Catal. A-Chem.* **248**, 226 (2006)
34. A.O. Ibadon, G.M. Greenway, Y. Yue, *Catal. Commun.* **9**, 153 (2008)
35. B. Cao, G. Li, H. Li, *Appl. Catal. B-Environ.* **194**, 42 (2016)
36. D.P. Debecker, B. Farin, E.M. Gaigneaux, C. Sanchez, C. Sassoeye, *Appl. Catal. A-Gen.* **481**, 11 (2014)
37. J. Feng, J. Sun, X. Liu, J. Zhu, Y. Xiong, S. Tian, *Environ Sci-Nano* **6**, 2241 (2019)
38. S.-B. He, P. Balasubramanian, Z.-W. Chen, Q. Zhang, Q.-Q. Zhuang, H.-P. Peng, H.-H. Deng, X.-H. Xia, W. Chen, *A.C.S. Appl. Mater. Inter.* **12**, 14876 (2020)
39. M.T. Atanasova, A. Vyalikh, U. Scheler, W.W. Focke, *Appl. Clay Sci.* **126**, 7 (2016)
40. Y. Huang, X. Ma, G. Liang, H. Yan, *Chem. Eng. J.* **141**, 1 (2008)
41. Z. Huang, P. Wu, B. Gong, X. Zhang, Z. Liao, P.-C. Chiang, X. Hu, L. Cui, *Appl. Clay Sci.* **142**, 128 (2017)
42. Z. Zhang, M. Jia, W. Jiao, B. Qi, H. Liu, *Constr. Build. Mater.* **171**, 33 (2018)
43. W. Liu, J. Yang, J. Cai, *Res. Chem. Intermediat.* **45**, 549 (2019)
44. H. Chen, C. Lu, H. Yang, *Appl. Clay Sci.* **199**, 105875 (2020)
45. Z. Sun, J. Xu, G. Wang, A. Song, C. Li, S. Zheng, *Appl. Clay Sci.* **184**, 105373 (2020)
46. H.H. Naing, K. Wang, P.P. Tun, G. Zhang, *Appl. Surf. Sci.* **491**, 216 (2019)
47. T. Bao, M.M. Dامتie, K. Wu, X.L. Wei, Y. Zhang, J. Chen, C.X. Deng, J. Jin, Z.M. Yu, L. Wang, R.L. Frost, *Appl. Clay Sci.* **176**, 66 (2019)
48. C.O. Ijagbemi, M.-H. Baek, D.-S. Kim, *J. Hazard. Mater.* **174**, 746 (2010)
49. K.G. Bhattacharyya, S.S. Gupta, *Desalination* **272**, 66 (2011)
50. D.S. Tong, Y.M. Zheng, W.H. Yu, L.M. Wu, C.H. Zhou, *Appl. Clay Sci.* **100**, 123 (2014)

51. F. Guo, X. Zhao, Y. Chen, R. Cai, H. Song, Q. Wang, Y. Huang, *Adv. Mat. Res.* **726–731**, 687 (2013)
52. S.-Y. Huang, S.-M. Chang, C. Yeh, *J. Phys. Chem. B* **110**, 234 (2006)
53. J.-H. Ma, Y.-Y. Feng, J. Yu, D. Zhao, A.-J. Wang, B.-Q. Xu, *J. Catal.* **275**, 34 (2010)
54. Y. Pu, J. Zhang, L. Yu, Y. Jin, W. Li, *Appl. Catal. A-Gen.* **488**, 28 (2014)
55. Z. Liu, V. Sriram, J.-Y. Lee, *Appl. Catal. B-Environ.* **207**, 143 (2017)
56. P. Singh, M.S. Hegde, *Chem. Mater.* **21**, 3337 (2009)
57. S. Sharma, Z. Hu, P. Zhang, E.W. McFarland, H. Metiu, *J. Catal.* **278**, 297 (2011)
58. A. Lebugle, U. Axelsson, R. Nyholm, N. Mårtensson, *Phys. Scripta* **23**, 825 (1981)
59. H. Nishikawa, T. Ihara, N. Kasuya, Y. Kobayashi, S. Takahashi, *Appl. Surf. Sci.* **479**, 1105 (2019)
60. C. Yin, T. Ye, Y. Yu, W. Li, Q. Ren, *Microchem. J.* **144**, 369 (2019)
61. D.H. Williams, I. Fleming, *Spectroscopic Methods in Organic Chemistry*, 5th edn. (McGraw-Hill Publishing Company, London, 1995), pp. 14–15
62. X. Xue, K. Hanna, M. Abdelmoula, N. Deng, *Appl. Catal. B-Environ.* **89**, 432 (2009)
63. H. Zhang, R.J. Bartlett, *Environ. Sci. Technol.* **33**, 588 (1999)
64. H. Wu, X. Dou, D. Deng, Y. Guan, L. Zhang, G. He, *Environ. Technol.* **33**(14), 1545 (2012)

Publisher's Note Springer Nature remains neutral with regard to jurisdictional claims in published maps and institutional affiliations.